IJIRSET
International Journal of Innovative Research in
SCIENCE | ENGINEERING | TECHNOLOGY

e-ISSN: 2319-8753 | p-ISSN: 2347-6710

INTERNATIONAL JOURNAL OF INNOVATIVE RESEARCH

IN SCIENCE | ENGINEERING | TECHNOLOGY

Volume 12, Issue 8, August 2023

INTERNATIONAL STANDARD SERIAL NUMBER INDIA

Impact Factor: 8.423

9940 572 462 | 6381 907 438 | ijirset@gmail.com | www.ijirset.com

International Journal of Innovative Research in Science, Engineering and Technology (IJIRSET)

|e-ISSN: 2319-8753, p-ISSN: 2320-6710| www.ijirset.com | Impact Factor: 8.423| A Monthly Peer Reviewed & Referred Journal |

|| Volume 12, Issue 8, August 2023 ||

| DOI:10.15680/IJIRSET.2023.1208072 |

Torsional Transient Response Analysis of Synchronous Motor driven Multistage Centrifugal Pump Using Finite Element Analysis

Ramana Podugu, J Suresh Kumar

Department of Mechanical Engineering, Jawaharlal Nehru Technological University, Hyderabad, Telangana, India

Professor, Department of Mechanical Engineering, Jawaharlal Nehru Technological University, Hyderabad, Telangana, India

ABSTRACT: The objective of this paper is to analyze the dynamic behaviour of the complex train which is a combination of multi-stage centrifugal pump-gear box-synchronous motor with VFD. Transient response analysis was performed on the complex train to analyze the dynamic torques and corresponding stresses during the engine startup. The purpose of a transient response analysis is to compute the dynamic behaviour of a structure subjected to time–varying excitation. The transient analysis evaluates the conditions on start-up which are continuously changing because of the time-varying torques from the motor load and acceleration of the system. The finite element technique that is Eigen value and Eigen vector method is used to find the torsional critical speeds and mode shapes. Finite element results were checked with theoretical calculations and it is observed that there is a good agreement between FEM results and hand calculations. In this paper, the peak dynamic stresses were compared with the fatigue limit of the material. At peak dynamic stresses, a number of start-ups were calculated based on the minor rule.

KEYWORDS: Torsional critical speeds, Holzer, Campbell, Eigenvector-Eigen value, Minor rule

I. INTRODUCTION

Since the early 1970s, the sub-synchronous resonance of the turbine generator has occurred twice in the Mohave power plant in America, which made shafts broken. From then on, the problems of the torsional vibration of the turbine generator were studied.

A chronological and informative discussion about the history of torsional vibration analysis is presented in Wilson [1]. It recognizes that early failures in marine and aeronautical drive trains presented the need for torsional vibration analysis. The Transfer Matrix method, the application of which has been described in detail in Pestel and Leckie [2] is an extension of Holzer's method. The method is modified by writing equations relating angular displacements to the internal forces in a matrix form and using complex variables to handle the damping. Using the modal approach as illustrated in Lund [3] and Childs [4-6], one can efficiently analyse the transient response of drive trains with many degrees of freedom. Eshleman [7] applied the modal approach in order to determine the torsional response of internal combustion engine drive trains that are subjected to constant and Pulsating torques. Anwar and Colsher [8] extended the modal approach to incorporate damping and backlash found in gears and couplings for torsional vibration analysis of large systems. They have presented a detailed discussion on the analysis of the start-up of drive trains employing a synchronous motor. The procedure for derivation of the element inertia and stiffness matrices has been outlined right from the basics in Rao [9]. These element matrices are then assembled to form the system inertia and stiffness matrices. Various methods for solving the system equations thus obtained are discussed in Bathe [10]. Squires [11] elicits the Finite Element method for determining torsional eigenvalues as well as eigenvectors, besides describing the modal method in which he uses undamped modes with truncation to determine the transient response.

Corbo and Malanoski [12][17] touch on almost all possible aspects, viz. modelling for torsional analysis, undamped and damped torsional natural frequency analyses, considerations for Variable Frequency Drives (VFDs), forced response analysis, transient analysis, etc. that should be considered while designing rotating machinery in order to avoid failures due to torsional vibration.Wachel and Szenasi [13] are another comprehensive resource of useful information on the modelling and analysis of drive trains for torsional vibration.

|e-ISSN: 2319-8753, p-ISSN: 2320-6710| www.ijirset.com | Impact Factor: 8.423| A Monthly Peer Reviewed & Referred Journal |

|| Volume 12, Issue 8, August 2023 ||

| DOI:10.15680/IJIRSET.2023.1208071 |

Corbo et al [14, 15] enumerate an explicit procedure for a design that can be used for avoiding problems arising due to torsional vibration in all forms of synchronous motor-driven turbomachinery. Their procedure, which includes an exhaustive practical example, lists detailed guidelines that a designer can follow while performing synchronous motor start-up analyses, determination of shaft size, surface finish, stress concentration, notch sensitivity, design safety factors, etc. They advocate the use of the strain life theory of failure as opposed to the conventional stress-life approach using Miner's rule to determine the life of the machine, defined in terms of the number of start-ups the machine can survive. Shigley and Mischke [16] give a generalized procedure for the design of shafts under fatigue loading. The relations for determining the values of various factors like those used to account for surface finish, size, etc. in the determination of a number of machine start-ups presented in this treatise have also been taken from [16].

Synchronous motors as pump drivers are normally used for higher-power applications. When the electric power is switched on, this type of motor generates a strong oscillating torque during starting because of slippage between the rotor and stator fields. During this period of time, the torsional system will be excited at several of its resonant frequencies. The excitation frequency varies from 120 cps at a standstill to zero at synchronous speed. Any torsional natural frequencies of the system within this frequency range (0 to 120 Hz) will be excited during the starting cycle as the pulsating torques pass through the critical frequency range.

Transient torques that arise in electrical motors can be separated into two categories; those that occur when the machine is running at operating speed and those that occur when the train is being started. Excitations are transient in nature, such as the starting of a synchronous motor, any kind of electrical fault, or torque ripples from the VFD motor.

The response amplitude and shaft stresses depend up on the resonant frequency, the average and dynamic torque when the system passes through each resonant frequency, the damping in the system, and the system load torques. The transient response is also affected by the acceleration time of the motor. For slow motor startups, the system will stay at a resonant frequency for a longer period of time allowing stresses to be amplified. Rapid acceleration through the resonances will minimize the amplification at resonant frequencies.

The initial shock to the torsional system is produced by the motor starting torque. The sudden application of the start-up torque shocks the shafting system and can cause many of its modes to be excited. The modes with the lowest dynamic stiffness will be most likely to respond. A resonance close to 120 Hz would be most undesirable since just at the initial shock the slip frequency is equal to twice the line frequency.

The voltage curve is directly related to the torque which includes both a steady-state torque component and a pulsating or dynamic torque component. The dynamic torque component is of primary importance since it produces the energy that would cause the vibrational response of the torsional natural frequency. The torsional natural frequencies should be located near frequencies having low dynamic torque components. Locating a torsional natural frequency in a region of high average torque during start-up can minimize the possibility of a response causing negative torque or backlash. Negative torque is particularly detrimental in geared systems.

A high acceleration rate through a torsional natural frequency is desirable since it will reduce the response magnification of the shafting system. The maximum response would be obtained if the system were running at the torsional natural frequency. The faster the motor passes through that frequency. the less opportunity the shafting system has to respond. The proper phase angle (90^0) must occur for the system to respond to its maximum. High acceleration rates minimize the time that this optimum phase angle occurs.

Vibratory exciting torques increase when twice slip frequency coincides with the lowest torsional system natural frequency somewhere during the running-up process. The level of vibratory shear stress that is reached depends on how fast the motor can pass the critical speed, how much damping is available in the shafting and of course, the size of the shafting at the weakest link, such as at the bearing journal, shaft end and coupling etc.

Obviously, if high acceleration rates are desirable, this would indicate a short start-up time is also desirable. All of these factors must be considered together to obtain the optimum location of the torsional natural frequencies for transient conditions. Fast startup time and high accelerations generally require high inertia torques which would introduce shocks into the system and be undesirable. Obviously, a balance between fast acceleration rates and initial torques must be obtained to find the optimum combination that will not severely limit the number of allowable startups.

|e-ISSN: 2319-8753, p-ISSN: 2320-6710| www.ijirset.com | Impact Factor: 8.423| A Monthly Peer Reviewed & Referred Journal |

|| Volume 12, Issue 8, August 2023 ||

| DOI:10.15680/IJIRSET.2023.1208071 |

The factors that must be considered in evaluating the optimum location of the transient resonances include the shape of the torque-speed curve, the initial starting torque of the motor, and the acceleration rate at the torsional natural frequency. The paper focuses on the torsional characteristics of synchronous motors during asynchronous starting.

II. METHOD OF CALCULATIONS

Traditionally, calculation of the transient torque is a lengthy and costly task, because it involves computerized integrations with very small steps and many degrees of freedom. There are many methods to calculate frequencies and mode shapes like the holzer method, transformation methods etc.
The vibratory motion of the system at this speed is represented by the modal equation:

A common analysis technique used for transient analysis is a numerical integration of the equation of motion in the form of a time-step solution. Beginning with the initial conditions of the motor at rest, the torque as determined from the start-up curve should be applied. The inertia of the system responds to this unbalanced torque and the system begins to rotate. At each step, the instantaneous values of pulsating torque, average torque, rotational speed, Inertia and damping are recalculated and the motor startup is simulated mathematically.

The time step for the numerical integration must be chosen to simulate the frequencies of interest. The basic equation of motion at time Tn+1 for the torsional system is:

$$[J]\left[\ddot{\theta}_{n+1}\right]+[C]\left[\dot{\theta}_{n+1}\right]+[K][\theta n+1]=\{T_{n+1}\} \qquad \ldots\ldots (1)$$

Where:

J = Mass Inertia Matrix

C = Damping matrix

K = Stiffness matrix

$\ddot{\theta}$ = Angular accelerati on matrix

$\dot{\theta}$ = Angular velocity matrix

θ = Angular displaceme nt matrix

T = Torque matrix

n = Counter for time step

$t_{n+1} = t_n + \nabla t;$

The angular acceleration, velocity and displacement can be accumulated using numerical integration methods like Backward Euler, ForwardEuler, Trapezoidal, runga kuta method etc.

III. FINITE ELEMENT COMPUTATION

3.1 Torsional modelling and calculation method:

The first step consists in discretizing the continuous stiffness and mass of inertia distribution to the torsional spring (stiffness) and torsional-mass elements. The stiffness and damping details of each step are shown in Table 3

Figure 1 presents the torsional mass-elastic system for the equipment arrangement with the gearbox. The arrangement evacuated in a four-branch system, whose low–speed branch operates at the motor's synchronous speed of 1832 rpm. Referring to this graph, the torsional elements are arranged sequentially from left to right. The balloons represent station-based inertia.

Branch#1 and Branch#2 contain low-speed drive components, namely the synchronous motor, low-speed gear and connected with low-speed coupling. The torsional mass elastic data for the high-speed shaft and motor shaft assemblies are contained in branches#3 and#4. branch#2 connected to branch#1 via a torsional spring at the end of shaft ends.

|e-ISSN: 2319-8753, p-ISSN: 2320-6710| www.ijirset.com | Impact Factor: 8.423| A Monthly Peer Reviewed & Referred Journal |

|| Volume 12, Issue 8, August 2023 ||

| DOI:10.15680/IJIRSET.2023.1208071 |

branch#3 connected to branch#2 via a torsional spring at the centerline of the pinion-to-gear mesh. Branch#4 is connected to branch#3 via a torsional spring at the ends of the coupling-to-shaft. The torsional stiffness values of these elements account for the flexibility of the geared systems, low-speed coupling and high-speed coupling. The inertia of the motor core, couplings, sleeves, seals, thrust collars and impellers are located at the respective stations. A multi-branch drive train, a dynamically equivalent system is developed internally referencing various branches to a single branch.

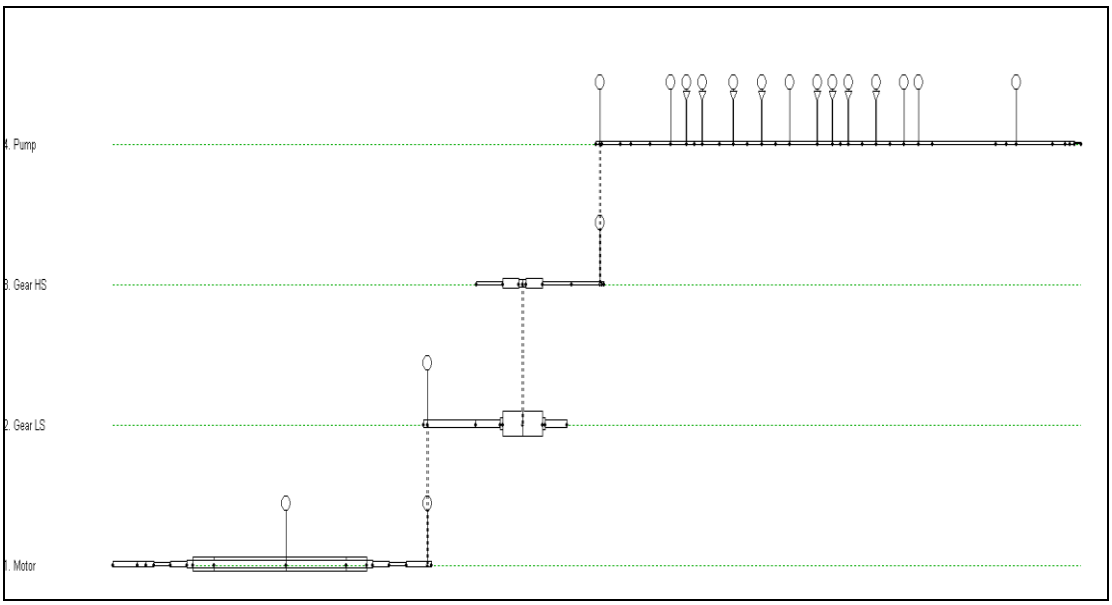

Fig 1. Torsional mass elastic system

3.2 Rotor data

Table 1: Rotor data

	Ref to Branch Speeds		Ref to branch #1 Speed		Description		Ref to Branch Speeds		Ref to branch #1 Speed		Description
S.No	Polar MI (Kg.m2)	Torsional stiffness (N.m/rad)	Polar MI (Kg.m2)	Torsional stiffness (N.m/rad)		S.No	Polar MI (Kg.m2)	Torsional stiffness (N.m/rad)	Polar MI (Kg.m2)	Torsional stiffness (N.m/rad)	
1	1.24E-02	5.83E+06	1.24E-02	5.83E+06	Shaft section	31	9.91E-03	3.29E+06	6.81E-02	2.26E+07	Shaft section
2	4.15E-03	1.75E+07	4.15E-03	1.75E+07	Shaft section	32	8.36E-03	2.98E+06	5.74E-02	2.05E+07	Shaft section
3	5.85E-03	2.47E+07	5.85E-03	2.47E+07	Shaft section	33	6.32E-04	3.94E+07	4.34E-03	2.71E+08	Coupling
4	4.86E-03	5.13E+06	4.86E-03	5.13E+06	Shaft section	34	5.83E-04	4.27E+07	4.00E-03	2.93E+08	Shaft section
5	2.01E-02	2.12E+07	2.01E-02	2.12E+07	Shaft section	35	0.00E+00	9.80E+05	0.00E+00	6.73E+06	Shaft section
6	1.33E-02	9.96E+07	1.33E-02	9.96E+07	Shaft section	36	2.07E-04	3.50E+06	1.42E-03	2.40E+07	Coupling
7	5.38E-01	3.63E+08	5.38E-01	3.63E+08	Shaft section	37	4.36E-04	2.94E+07	2.99E-03	2.02E+08	Shaft section
8	1.88E+00	1.04E+08	1.88E+00	1.04E+08	Disc	38	5.47E-03	4.56E+06	3.75E-02	3.13E+07	Shaft section
9	1.56E+00	1.25E+08	1.56E+00	1.25E+08	Shaft section	39	3.11E-03	8.01E+06	2.13E-02	5.50E+07	Shaft section
10	5.38E-01	3.63E+08	5.38E-01	3.63E+08	Shaft section	40	4.06E-03	3.39E+06	2.79E-02	2.33E+07	Shaft section
11	1.33E-02	9.96E+07	1.33E-02	9.96E+07	Shaft section	41	6.07E-03	4.10E+06	4.17E-02	2.81E+07	Disc
12	1.95E-02	2.18E+07	1.95E-02	2.18E+07	Shaft section	42	9.43E-03	2.64E+06	6.47E-02	1.81E+07	Disc
13	5.15E-03	4.84E+06	5.15E-03	4.84E+06	Shaft section	43	5.74E-03	5.55E+06	3.94E-02	3.81E+07	Shaft
14	1.50E-02	9.62E+06	1.50E-02	9.62E+06	Disc	44	4.47E-03	7.14E+06	3.07E-02	4.90E+07	Disc
15	2.93E-03	4.94E+07	2.93E-03	4.94E+07	Shaft section	45	9.38E-03	3.40E+06	6.44E-02	2.33E+07	Disc
16	0.00E+00	2.08E+06	0.00E+00	2.08E+06	Disc	46	9.38E-03	3.48E+06	6.44E-02	2.39E+07	Disc
17	7.41E-03	1.25E+08	7.41E-03	1.25E+08	Coupling	47	9.38E-03	3.48E+06	6.44E-02	2.39E+07	Disc
18	8.62E-02	1.07E+07	8.62E-02	1.07E+07	Shaft section	48	5.27E-03	6.32E+06	3.62E-02	4.34E+07	Disc
19	5.20E-02	2.52E+07	5.20E-02	2.52E+07	Shaft section	49	5.27E-03	6.32E+06	3.62E-02	4.34E+07	Disc
20	7.13E-02	2.29E+09	7.13E-02	2.29E+09	Shaft section	50	9.38E-03	3.48E+06	6.44E-02	2.39E+07	Disc
21	6.48E+00	4.84E+09	6.48E+00	4.84E+09	Shaft section	51	9.38E-03	3.48E+06	6.44E-02	2.39E+07	Disc
22	6.48E+00	4.84E+09	6.48E+00	4.84E+09	Shaft section	52	9.28E-03	3.44E+06	6.37E-02	2.36E+07	Disc
23	7.28E-02	2.24E+09	7.28E-02	2.24E+09	Shaft section	53	1.87E-02	1.33E+06	1.28E-01	9.14E+06	Disc
24	4.63E-02	2.83E+07	4.63E-02	2.83E+07	Shaft section	54	3.04E-03	8.20E+06	2.08E-02	5.63E+07	Shaft section
25	0.00E+00	6.54E+08	0.00E+00	6.54E+08	Coupling	55	3.04E-03	8.20E+06	2.08E-02	5.63E+07	Shaft section
26	8.87E-03	3.68E+06	6.09E-02	2.52E+07	Shaft section	56	7.90E-03	1.74E+06	5.43E-02	1.20E+07	Shaft section
27	1.13E-01	1.26E+08	7.74E-01	8.68E+08	Shaft section	57	1.39E-03	2.60E+06	9.54E-03	1.79E+07	Disc
28	1.93E-02	4.25E+08	1.33E-01	2.92E+09	Shaft section	58	3.65E-04	4.62E+06	2.51E-03	3.17E+07	Shaft section
29	1.93E-02	4.25E+08	1.33E-01	2.92E+09	Shaft section	59	3.65E-04	4.62E+06	2.51E-03	3.17E+07	Shaft section
30	1.13E-01	1.26E+08	7.74E-01	8.68E+08	Shaft section	60	1.21E-05	9.11E+04	8.34E-05	6.25E+05	Shaft section

|e-ISSN: 2319-8753, p-ISSN: 2320-6710| www.ijirset.com | Impact Factor: 8.423| A Monthly Peer Reviewed & Referred Journal |

|| Volume 12, Issue 8, August 2023 ||

| DOI:10.15680/IJIRSET.2023.1208071 |

3.3 Material data

Various steel-grade materials are used for the pump; the motor, high-speed shaft and low-speed shaft are shown in Table 2.

Table 2. Material properties

Component	Material Grade	Young's Modulus	Shear Modulus	Density	Yield stress	Tensile strength	Fatigue Strength
		Mpa	Mpa	Kg/m3	Mpa	Mpa	Mpa
Pump Shaft	Steel	2.00E+05	8.50E+05	7.80E+03	758	931	465
Motor Shaft	Steel	2.00E+05	8.50E+05	7.80E+03	758	931	465
HS shaft	Steel	2.00E+05	8.50E+05	7.80E+03	896	1103	552
Ls shaft	Steel	2.00E+05	8.50E+05	7.80E+03	896	1069	534

IV. CHARACTERISTIC CURVES

The motor and pump (load) characteristic curves used for the analysis were taken as shown in Figure 2. Note that the pump was started with the valve closed, and hence, 100% full load torque does not appear on the pump (load) torque curve. If the pump had been started with its valve open, the full load torque would have been reached around the synchronous speed of the motor.

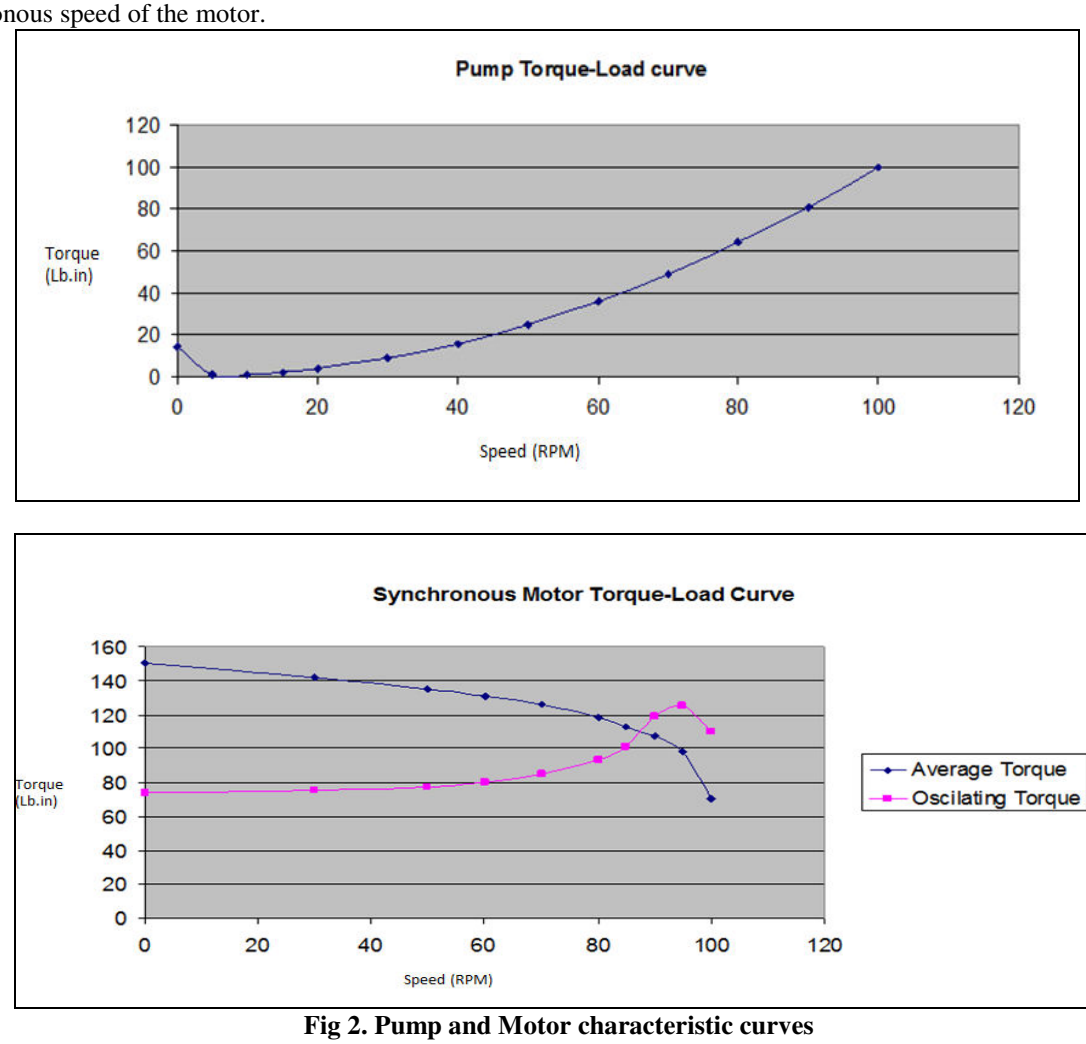

Fig 2. Pump and Motor characteristic curves

|e-ISSN: 2319-8753, p-ISSN: 2320-6710| www.ijirset.com | Impact Factor: 8.423| A Monthly Peer Reviewed & Referred Journal |

|| Volume 12, Issue 8, August 2023 ||

| DOI:10.15680/IJIRSET.2023.1208071 |

V. EVALUATION OF TORSIONAL FREQUENCIES AND MODES

The number of degrees of freedom possessed by the system is equal to the number of discs in the model. The number of non-trivial natural frequencies that can be obtained for such a system is, thus, one less than the number of discs in the model. Each natural frequency has an associated mode shape which describes the shape of the shaft twists during free vibration. Representative mode shapes are shown in Fig.3 and Fig.4. The mode shape represents the relationship between the displacements at the various discs. In this work, results are validated to avoid errors and unexpected results. The first fundamental frequency is calculated by approximating a two-disc system by adding together all of the inertia and stiffnesses on each side of the coupling. The mode shapes are checked if they obey the conservation of angular momentum.

Table 3. Calculated Natural frequencies

Mode No	Frequency (RPM)	Mode No	Frequency (RPM)	Mode No	Frequency (RPM)
1	2792	10	59399	19	125247
2	5688	11	73190	20	218543
3	18780	12	79535	21	225879
4	29229	13	86443	22	233545
5	31189	14	96301	23	234187
6	36847	15	96316	24	249178
7	44688	16	104344	25	262177
8	45564	17	109513		
9	56279	18	111339		

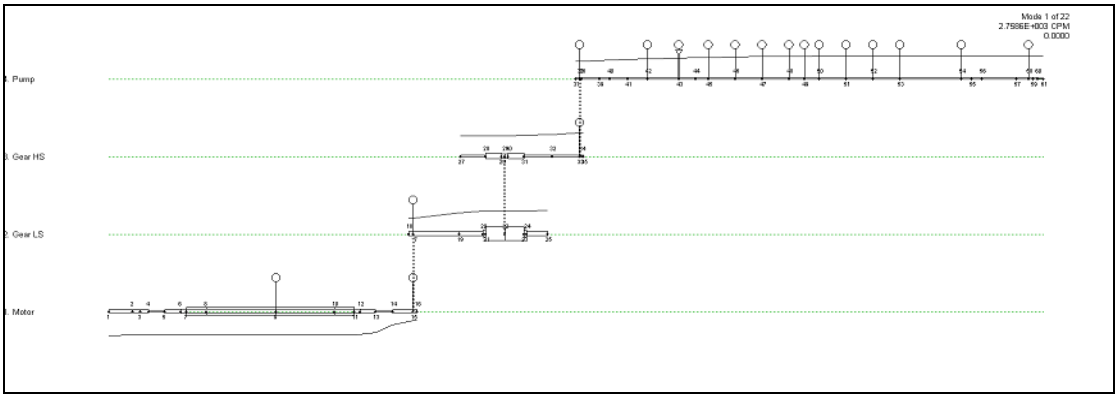

Fig 3. First Mode Shape

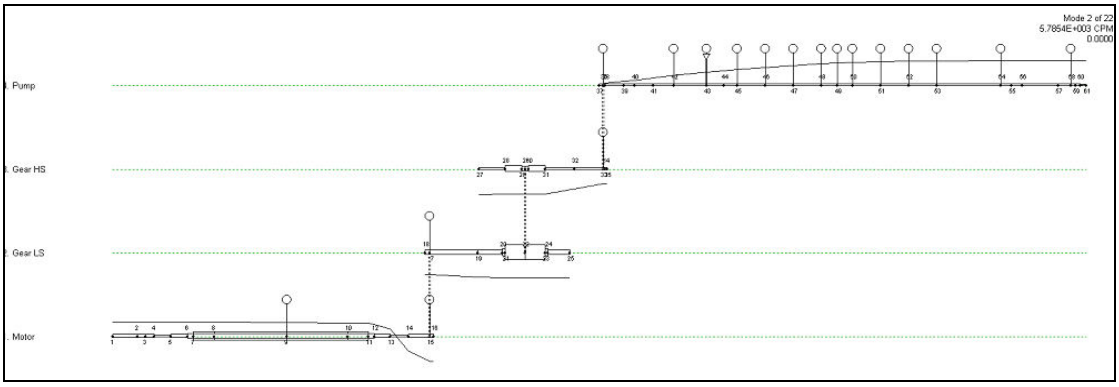

Fig 4. Second Mode shape

|e-ISSN: 2319-8753, p-ISSN: 2320-6710| www.ijirset.com | Impact Factor: 8.423| A Monthly Peer Reviewed & Referred Journal |

|| Volume 12, Issue 8, August 2023 ||

| DOI:10.15680/IJIRSET.2023.1208071 |

VI. RESULTS AND DISCUSSIONS

6.1 Generation of Campbell diagram

Campbell diagrams can be very helpful to identify all potential resonant points. A representative diagram for a Campbell diagram is depicted in Fig.5. Figure 5 presents a Campbell diagram for a typical synchronous motor-driven train. This diagram provides a graphic overview of the rotor system's torsional natural frequencies and its corresponding frequencies of potential excitation. In this example, the first three torsional natural frequencies are given along with the excitation line corresponding to double slip frequency. it can be easily seen that motor excitations interfere with the first three natural frequencies, which are all below twice the line frequency (120 Hz). The motor speeds at which frequency with the natural frequency occur can be calculated as follows.

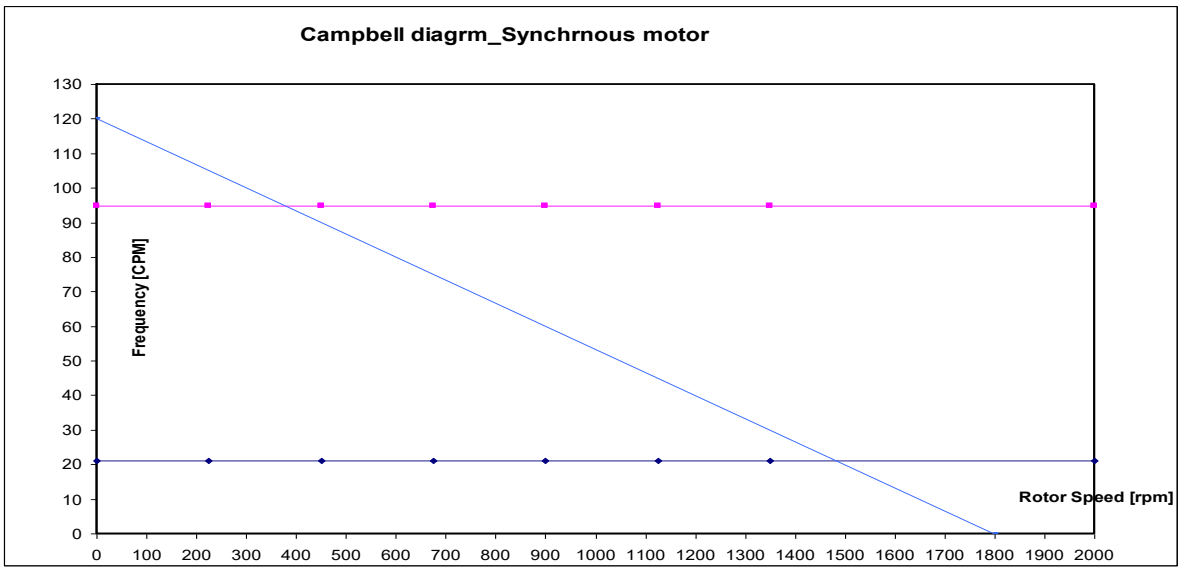

Fig.5. Campbell diagram

6.2 Stress results

High transient stresses (above the endurance limit) cause premature failure of the shafts and consequently limit the allowed number of start-ups before a failure would occur. For this reason, the transient stresses must be calculated and compared to the endurance limit stress. The transient stresses, however, must be sufficiently low to allow an acceptable number of starts. If the transient stresses exceed the endurance limit, then the cumulative fatigue concept should be applied to sum the number of cycles in which the stresses exceed the endurance limit to determine how many starts can be allowed for the system.

The cumulative fatigue theory basically defines how many allowable cycles of a certain level of stress can be tolerated before failure would occur. This is based upon a plot of stress versus a number of cycles (S-N curve) which defines the stress at which a failure should occur. The allowed number of cycles for a particular stress can be determined based on the S-N curve. If a fraction of these cycles has been used in the transient start-up, then the total startups of the system before a shaft failure would be expected can be defined. Since stress levels vary both in amplitude and frequency, a more complex calculation must determine the fraction of the total fatigue which has occurred. These stress levels must be analyzed for each cycle to determine the percentage of cumulative fatigue and then the allowable number of start-ups can be calculated using the S-N curve.

The allowable number of start-ups can be calculated using the cumulative fatigue method which is popularly known as the minor rule as shown in equation (2)

|e-ISSN: 2319-8753, p-ISSN: 2320-6710| www.ijirset.com | Impact Factor: 8.423| A Monthly Peer Reviewed & Referred Journal |

|| Volume 12, Issue 8, August 2023 ||

| DOI:10.15680/IJIRSET.2023.1208071 |

$$\frac{1}{q} = \sum_{i=1}^{n} \frac{N_i}{n_i} \qquad \text{..... (2)}$$

Where, $\frac{1}{q}$ = Allowable number of start-ups

N_i =Number of cycles to failure at σ_i

n_i =Actual number of cycles at σ_i

σ_i =Stress at i^{th} cycle.

The motor shaft Campbell diagram of the figure was then generated to determine the potential resonances triggered by the synchronous motor excitation. Thus, the transient response analysis focused on simulating the responses at the first two natural frequencies with the fundamental being the primary concern.

Fig.6 to Fig.9 represents dynamic torques obtained from FEA calculations. These are the results of the transient analysis consisting of the time histories of the torque in all four shafts. These plots revealed the response as the system passed through the second natural frequency resonance point.

Examination of the figure reveals that the torques are fairly smooth up until resonance is approached. Once the resonance zone is entered at about 1.5 sec, the ripple rises steadily until it reaches a peak at about 0.5 seconds. Peak dynamics torques are calculated from the dynamic torques obtained from FEA calculations. Fatigue calculations are performed to find the fatigue life of the shafts. From the fatigue calculations, it is observed that the life of the shaft is 22284 cycles at the coupling end of the pump shaft.

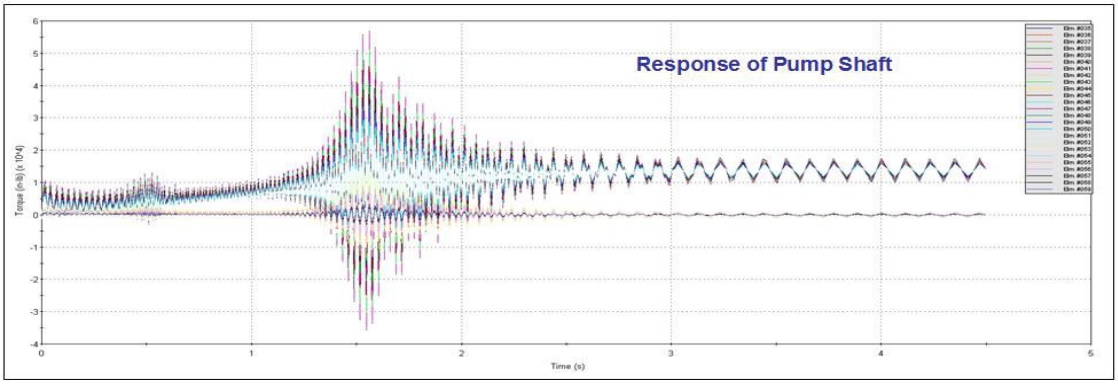

Fig.6. Dynamic Torque for Pump Shaft

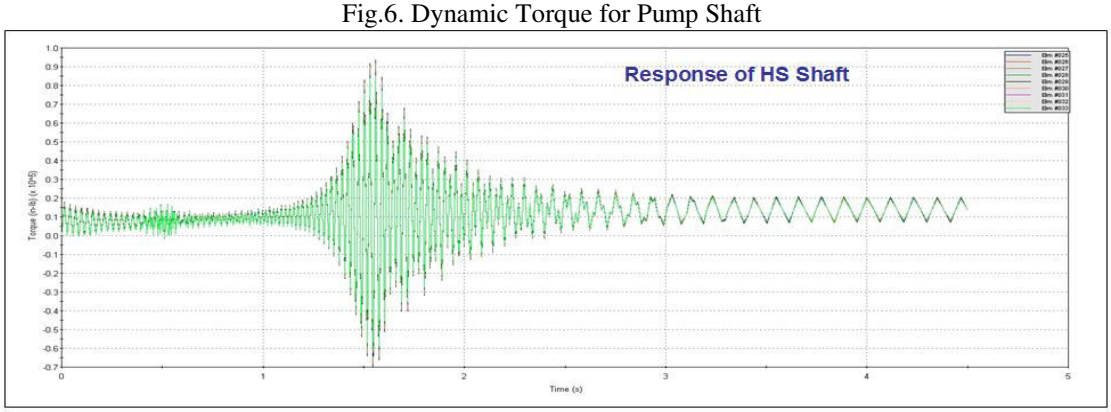

Fig.7. Dynamic Torque for High-Speed Shaft

|e-ISSN: 2319-8753, p-ISSN: 2320-6710| www.ijirset.com | Impact Factor: 8.423| A Monthly Peer Reviewed & Referred Journal |

|| Volume 12, Issue 8, August 2023 ||

| DOI:10.15680/IJIRSET.2023.1208071 |

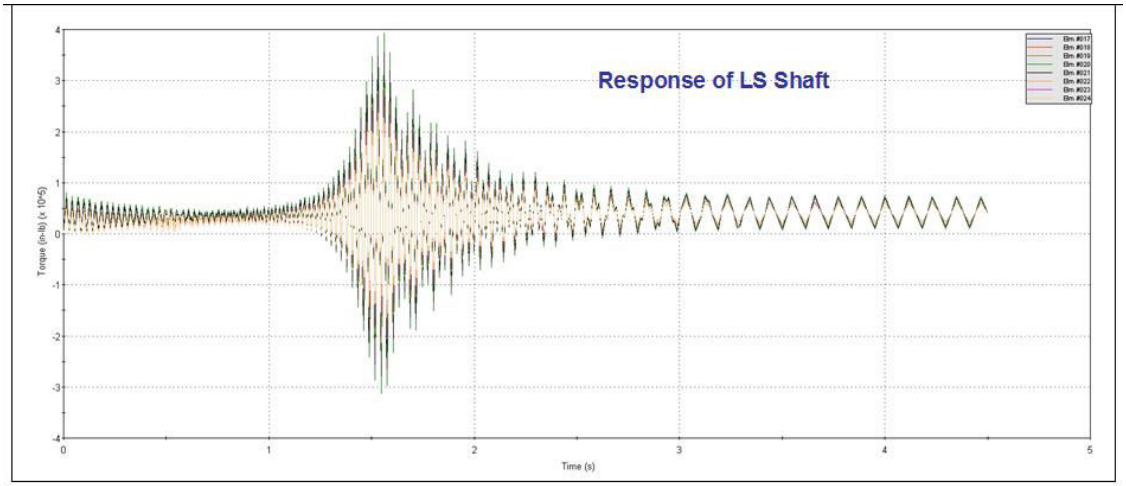

Fig.8. Dynamic Torque for Low-Speed Shaft

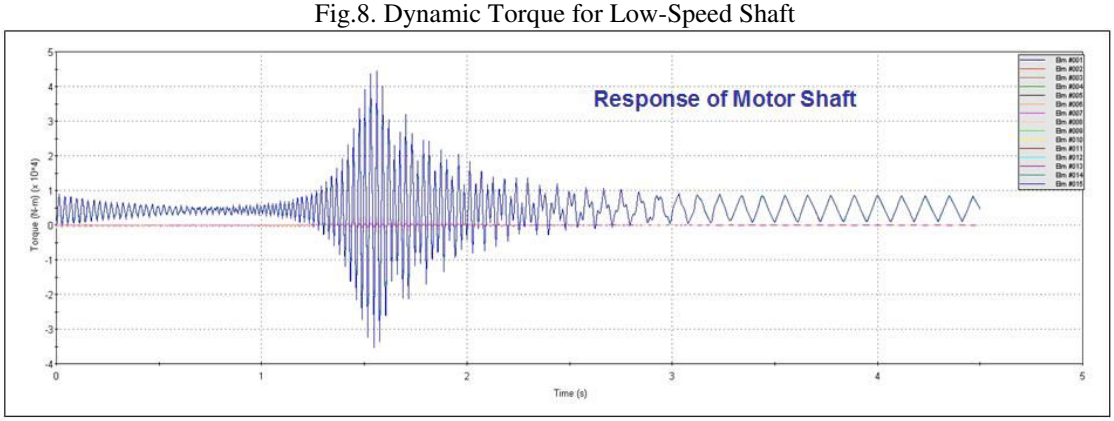

Fig.9. Dynamic Torque for Motor Speed Shaft

VII. CONCLUSIONS

A transient torsional analysis is necessary to design a reliable synchronous motor system. During the synchronous motor start-up with a variable power supply system, different torsional natural frequencies could be excited due to resonance with power supply harmonics. The degree of resonance of different natural frequencies with power supply harmonics is different on the rate of acceleration and the different harmonic content of the pulsation torque generated by the motor during start-up. The most desirable rate of acceleration could be determined through transient response analysis of the system. The results obtained from the response analyses could be used to determine shaft shear stresses. Performing fatigue damage analyses to ensure the reliability of the torsional system through designing for an adequate number of start-ups has been discussed in this paper. Changes required to ensure to result in a reliable system could also be ensured through such analyses during the design stage.

REFERENCES

[1] Wilson, W. K., 1956, Practical Solution of Torsional Vibration Problems, Volume One: Frequency Calculations, 3rd Ed., John Wiley and Sons, New York, pp. xiii–xxxii..
[2] Pestel, E.C. and Leckie, F. A., 1963, Matrix Methods in Elastomechanics, McGraw-Hill Book Company, New York, pp. 51–129.
[3] Lund, J. W., 1974, "Modal Response of a Flexible Rotor in Fluid-Film Bearings, "ASME Journal of Engineering for Industry, Vol. 96, No. 2, pp. 525-533..
[4] Childs, D. W., 1974, "A Rotor Fixed Model Simulation Model for Flexible Rotating Equipment," ASME Journal of Engineering for Industry, Vol. 96, No. 2,pp. 359-369.

|e-ISSN: 2319-8753, p-ISSN: 2320-6710| www.ijirset.com | Impact Factor: 8.423| A Monthly Peer Reviewed & Referred Journal |

|| Volume 12, Issue 8, August 2023 ||

| DOI:10.15680/IJIRSET.2023.1208071 |

[5] Childs, D. W., 1975, "Two Jeffcott Based Modal Simulation Models for Flexible Rotating Equipment." ASME Journal of Engineering for Industry, Vol. 97, No. 3,pp. 1000-1014.
[6] Childs, D. W., 1976, "A Modal Transient Rotor Dynamic Model for Dual Rotor Jet Engine Systems," ASME Journal of Engineering for Industry, Vol. 98, No. 3, pp.876-882.
[7] Eshleman, R. L., 1974, "Torsional Resonance of Internal Combustion Engines,"ASME Journal of Engineering for Industry, Vol. 96, pp. 441-449
[8] Anwar, I. and Colsher, R., 1979, "Computerized Time Transient Torsional Analysis of Power Trains," ASME Paper 79-DET-74, ASME Design Engineering Division.
[9] Rao, S. S., 1995, Mechanical Vibrations, Addison-Wesley Publishing Company, Boston, MA, pp. 725-749..
[10] Bathe, K. J., 1996, Finite Element Procedures, Prentice Hall, Englewood Cliffs,NJ, pp. 887-937.
[11] Squires, D. C., 1984, “Transient Analysis of Torsional Vibrations in Rotor Systems”, M.S. Thesis, Univ. of Virginia, Charlottesville.
[12] Corbo, M. A. and Malanoski, S. B., 1996, “Practical Design Against Torsional Vibration,” Proceedings, 25th Turbomachinery Symposium, Texas A&M Univ., College Station.
[13] Wachel, J. C. and Szenasi, F. R., 1993, “Analysis of Torsional Vibrations in Rotating Machinery,” Proceedings, 22nd Turbomachinery Symposium, Texas A&M Univ., College Station.
[14] Corbo, M. A. and Cook, C.P., 2000, "Torsional Vibration Analysis of Synchronous Motor-driven Turbo machinery," Proceedings, 29th Turbomachinery Symposium, Texas A&M Univ., College Station.
[15] Corbo, M. A., Cook, C. P., Yeiser, C. W. and Costella, M. J., 2002, “Torsional Vibration Analysis and Testing of Synchronous Motor-driven Turbomachinery”, Proceedings, 31st Turbomachinery Symposium, Texas A&M Univ., College Station.
[16] Shigley, J. E. and Mischke, C. R., 2001, Mechanical Engineering Design, 6th Ed., McGraw-Hill Book Company, New York
[17] Ramana Podugu.,2011,” A modal approach for vibration analysis and condition monitoring of a centrifugal pump”, Int. J. Eng. Sci. Technol. (IJEST), 3 (8) (2011), pp. 6335-6344, ISSN: 0975-5462.

INNO SPACE
SJIF Scientific Journal Impact Factor

Impact Factor: 8.423

doi cross ref

ISSN INTERNATIONAL STANDARD SERIAL NUMBER INDIA

निस्केयर NISCAIR

INTERNATIONAL JOURNAL OF INNOVATIVE RESEARCH

IN SCIENCE | ENGINEERING | TECHNOLOGY

9940 572 462 6381 907 438 ijirset@gmail.com

www.ijirset.com

Scan to save the contact details